

## Photoemission from surface states and surface resonances on the (100), (110), and (111) crystal faces of aluminum

G. V. Hansson and S. A. Flodström

*Department of Physics and Measurement Technology, Linköping University, S-581 83 Linköping, Sweden*

(Received 5 January 1978)

The angular-resolved energy distributions for photoelectrons emitted from the (100), (110), and (111) crystal faces of aluminum are presented for photon energies in the range 7.0–11.6 eV. The emission in this photon energy range is dominated by surface photoemission excited by the normal optical field or the surface-plasmon field. Three structures in the spectra are identified as emission from electronic surface states that have been predicted in theoretical calculations. Two of these surface-state bands, seen in emission from the (100) and (110) crystal faces, are associated with the *sp* band gap around the *X* point in  $\vec{k}$  space. We interpret a structure in the emission from the (111) crystal face as due to a surface resonance band also associated with the *sp* band gap around the *X* point. No conclusive evidence for the existence of structures in the spectra due to direct transitions in the bulk has been obtained.

### I. INTRODUCTION

The technique of angular-resolved photoemission has earlier been applied to the study of electronic states of single crystals of numerous materials.<sup>1</sup> It has been successful in the examination of bulk and surface electronic structure for noble and transition metals, while there have been only comparatively few measurements reported on aluminum and other nearly-free-electron metals.<sup>2</sup> This is surprising, since there are several theoretical papers which predict the existence of surface states on the (100), (110), and (111) crystal faces of aluminum.<sup>3–7</sup> Most previous photoemission studies on aluminum have been focused on either the polarization dependence of the yield at different photon energies<sup>8,9</sup> or the oxidation process.<sup>10–12</sup> Gartland and Slagsvold<sup>2</sup> have measured the angular-resolved photoemission from the Al(100) crystal face using resonance radiation (11.7, 16.8, and 21.2 eV). They reported emission from a two-dimensional band of surface states which connects to a surface resonance band going up to the Fermi level. In this paper we confirm their results and we also report emission from two different surface-state bands on the Al(110) crystal face and one surface resonance band on the Al(111) crystal face.

We also discuss the contribution to electron emission by decaying surface plasmons as compared to bulk photoemission and surface photoemission through the optical field. It is known that the decay of surface plasmons gives a considerable contribution to the yield in photoemission<sup>8,9,13</sup> and it is not negligible in secondary-electron emission.<sup>14</sup> For photoemission, this mechanism varies strongly with photon energy, being most important close to the surface-plasmon energy. By recording spectra at different photon energies, and varying the angle of light incidence we have found

that the surface-plasmon field is the main excitation source at energies around the plasmon energy  $\hbar\omega_{sp}$  (10.5 eV for aluminum).

An attempt was also made to correlate our experimental results with the bulk band structure. The energy positions of peaks due to direct transitions in the bulk were obtained using the band structure calculated by Snow.<sup>15</sup>

### II. THEORY

The complete theoretical description of the photoemission process has not yet been achieved. Several authors<sup>16,17</sup> have derived a Golden Rule expression for photoemission within the framework of the independent-particle model. For cases in which hole damping may be neglected, the photocurrent at the detector can be written<sup>17</sup>

$$j(\vec{R}, E) \sim \sum_{\text{occupied } i} \delta(E - \hbar\omega - E_i) |\langle \psi_f | \hat{O} | \psi_i \rangle|^2, \quad (1)$$

where the operator  $\hat{O}$  is defined by

$$\hat{O}(\vec{x}) = \frac{1}{2} [\vec{A}(\vec{x}) \cdot \vec{p} + \vec{p} \cdot \vec{A}(\vec{x})]. \quad (2)$$

The wave function  $\psi_f$  needed to calculate the matrix elements is a time-reversed low-energy electron-diffraction (LEED) function.

Although not quite correct,<sup>18</sup> it is very useful to separate different terms in the operator when discussing different mechanisms for photoemission. The total matrix element for the photoemission process then appears as<sup>18</sup>

$$M_{fi} \approx (-i/\omega) (\langle f | \vec{A} \cdot \vec{\nabla} V_B | i \rangle + \langle f | \vec{A} \cdot \vec{\nabla} V_s | i \rangle) - \frac{1}{2} i \hbar \langle f | (\partial \vec{A} / \partial z) | i \rangle. \quad (3)$$

The direction of the surface normal is given by  $\hat{z}$ , while  $V_s$  is the surface-barrier potential and  $V_B$  is the bulk potential. The first term gives the

bulk photoemission which, in the case of weak damping, is described as being due to direct inter-band transitions. The remaining two terms are responsible for the surface-induced photoemission and are called the surface-potential term and the surface-field term, respectively.

The importance of the surface-field term at high photon energies has not been established experimentally, while for photon energies below the plasmon energy it is very important. For a correct description of the surface-potential term, it is necessary to know the microscopical variation of the vector potential  $\vec{A}$ . Feibelman<sup>19</sup> has calculated the surface-photoelectric effect self-consistently using the jellium model. He showed that the contribution from the surface-photo effect depends strongly on photon energy. A peak in the yield was obtained in the interval  $0 < \omega < \omega_p$ . This peak moves closer to  $\omega_p$  and decreases in magnitude as the steepness of the surface potential barrier increases.

Pendry<sup>20</sup> has calculated the angular-resolved photoemission considering the bulk potential and surface-potential terms assuming a constant vector potential ( $\vec{A}$  vector). For the photon energies used (11.7, 16.8, and 21.2 eV), the emission in the investigated directions is nearly all due to the surface-potential term, since the effective potential of the ion cores is weak.

A further complication in photoemission from nearly-free-electron metals is the effect of surface roughness. It is well known that the photoelectric yields for aluminum and magnesium have large peaks, when the photon energies are close to the surface-plasmon energies.<sup>8,9</sup> The height of these peaks is strongly dependent on the surface roughness and can in fact be used as a measure of this quantity.<sup>20</sup> The increase in the yield is due to the deexcitation of surface plasmons by the emission of electrons. A perfect surface does not couple the incident light to surface plasmons, but the existence of surface roughness mediates surface-plasmon creation. Even for the smoothest surfaces of free-electron-like metals used in photoemission, the roughness-induced surface plasmons have been important as excitation source.<sup>8,21</sup>

An important feature of the roughness-induced surface-plasmon excitation is that it is not very sensitive to the polarization of the incident light. The weak polarization dependence observed is due to the varying coupling between the incident light and the surface plasmons and is not an inherent property of the surface-plasmon field. The surface-plasmon field can be described formally as the optical field of the light coming in at an complex angle of incidence at grazing incidence, i.e., the surface-plasmon field is *p*-polarized with a major component of the  $\vec{A}$  vector normal to the

surface.<sup>22</sup> Hence, for a real surface, there is an increase in the yield at the surface-plasmon energy due to surface photoemission excited by an  $\vec{A}$  vector normal to the surface, independent of the polarization or angle of incidence of the light.

A major objective of this study has been to check the bulk and surface energy band structure of aluminum. We have performed a four-orthogonalized-plane-wave band calculation including three free-electron bands. The parameters were chosen to be  $V_{200} = 0.0437$  Ry,  $V_{111} = 0.0146$  Ry, and  $m^* = 1.06m_0$ . With this choice of parameters, the band calculation is within 0.1 eV from the self-consistent augmented-plane-wave calculation of Snow<sup>15</sup> for states below the Fermi level. Using this band structure we have calculated the angular variation of peak energy positions assuming direct transitions in the bulk.

Caruthers *et al.*<sup>4-6</sup> have made calculations of the electronic surface states on the Al(100), Al(110), and Al(111) crystal faces, predicting surface states on all crystal faces. Their results for the Al(111) crystal face have been confirmed in a self-consistent pseudopotential calculation by Chelikovsky *et al.*<sup>7</sup> These calculations have been concentrated on the existence of surface states within the absolute gaps between bands of the same symmetry. There are regions of  $k_{||}$  values where the projected band gap between two bulk energy bands is intersected by the projection of a third bulk energy band. If all three bands have the same symmetry there will be mixing of the bands due to the presence of the surface. The effect of the mixing with the third band is then to "fill the band gap" between the first two bands. Sometimes new band gaps are created.<sup>4-6</sup> If the mixing is small, it is possible to get surface resonances within these "filled band gaps." Gartland and Slagsvold<sup>2</sup> have shown that the dominant feature in emission from the Al(100) crystal face at certain angles can be accounted for by such a surface resonance. By making projections of the band gaps on to the three planes investigated, we show that surface resonances or surface states originating from the widest band gap (around the *X* point) describe features of our spectra on all surfaces in a satisfactory manner.

### III. EXPERIMENTAL

The experimental setup has been described in fuller detail elsewhere.<sup>22</sup> The experiments were performed in an ultra high vacuum chamber connected to a McPherson Model No. 225 monochromator. Our light source is a Hinteregger-type hydrocarbon discharge lamp. The 127° cylindrical deflection analyzer has an energy resolution of 2%, i.e.,  $\Delta E \leq 0.2$  eV. The electrons enter the analyzer in

a near-conical distribution with a mean cone angle of  $\pm 4^\circ$ .

The samples were high-purity single crystals of aluminum which had been spark cut, mechanically polished, and electropolished according to standard procedures. The orientations of the surface normals were checked using the channeling pattern technique in a scanning electron microscope and found to be within  $2^\circ$  of the desired symmetry directions. The channeling-pattern technique was also used to check the surface order before and after the measurements.

The samples were cleaned in ultrahigh vacuum by repeated cycles of argon sputtering and annealing at  $350^\circ\text{C}$ . Each crystal was sputtered for more than 120 min (600 V,  $10\ \mu\text{A}/\text{cm}^2$ ). In the measurement on the Al(100) crystal face, the base pressure in the vacuum chamber was  $5 \times 10^{-11}$  Torr, while it was  $8 \times 10^{-10}$  Torr in the measurements on the Al(110) and Al(111) crystal faces. With this rather high pressure, contamination was evident as changes in the spectra about 5 h after a cleaning cycle.<sup>23</sup> All spectra shown have been taken less than 4 h after a cleaning cycle.

The variable angles in the setup are the angle of light incidence  $\theta_i$ , the polar emission angle of the analyzed electrons in the plane of incidence  $\theta_e$ , and the azimuthal angle of the sample  $\phi$ . Two sets of measurements have been performed. In the first, we kept all angles fixed and measured the normal emission for different photon energies. Within such a series the intensities were normalized arbitrarily without relating them to the photon flux. The second independent set was obtained by fixing photon energy, angle of light incidence, and azimuthal angle, and then varying the polar angle of the analyzer. These angular-resolved energy-distribution curves (AREDC's) show the true relative intensities, i.e., intensities can be compared within one set of curves.

#### IV. RESULTS

##### A. Al(100)

The emission in the normal direction for different photon energies is shown in Fig. 1. The dominant feature is a peak A, located about 2.75 eV below the Fermi level for all photon energies high enough to emit electrons with this initial energy. All spectra also show a very similar nearly linear increase in intensity from  $-1.7$  eV towards the Fermi energy called structure B. The lack of changes in the AREDC's with photon energy indicates that direct transitions in the bulk are not important. Comparison with the bulk band structure also shows that structures A and B cannot be due to direct transitions. What we see are features

in the initial density of states for  $\vec{k}_\parallel = 0$ , modulated by a factor which includes the matrix elements.

The band calculation shows that there is a band gap in the [100] direction between  $-2.0$  and  $-3.2$  eV, i.e., the position of peak A is close to the middle of the band gap. As Gartland and Slagsvold did, we interpret this peak as emission from a surface state in the X-point band gap. We have also measured the emission for different polar angles in the two symmetry planes (010) and (011). Figure 2 shows the AREDC's in the (011) plane for polar angles in the range  $-30^\circ$  to  $75^\circ$ . Peak A shows a very strong and symmetric dispersion passing the Fermi level at about  $45^\circ$ . Within the experimental accuracy the dispersion in the (010) plane was the same. Assuming a parabolic form of the dispersion curve, the best least-squares fit to experiment gives an effective mass of  $m^* = 1.02 \pm 0.05$  in units of the free-electron mass.

In Fig. 3, the peak position is plotted as function of  $\vec{k}_\parallel$  for both measurement series, assuming a work function of 4.41 eV.<sup>24</sup> Error bars corresponding to a maximum total uncertainty of  $5^\circ$  in

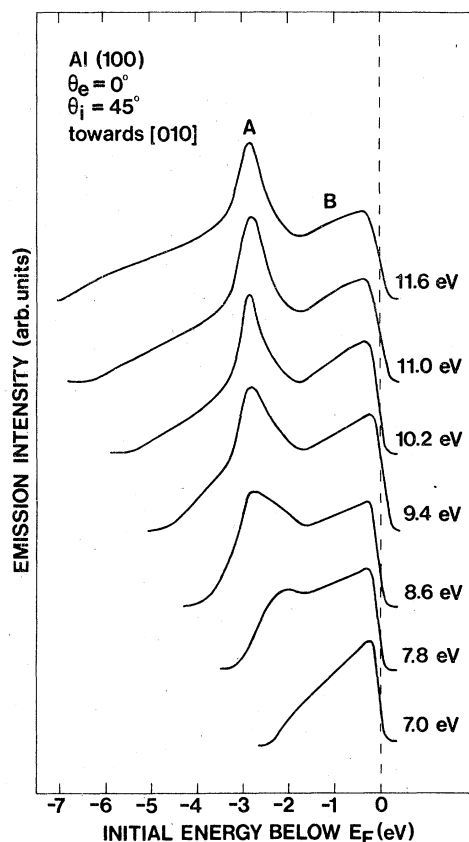


FIG. 1. Experimental spectra of photoelectrons emitted normal to the (100) crystal face for photon energies between 7.0 and 11.6 eV.

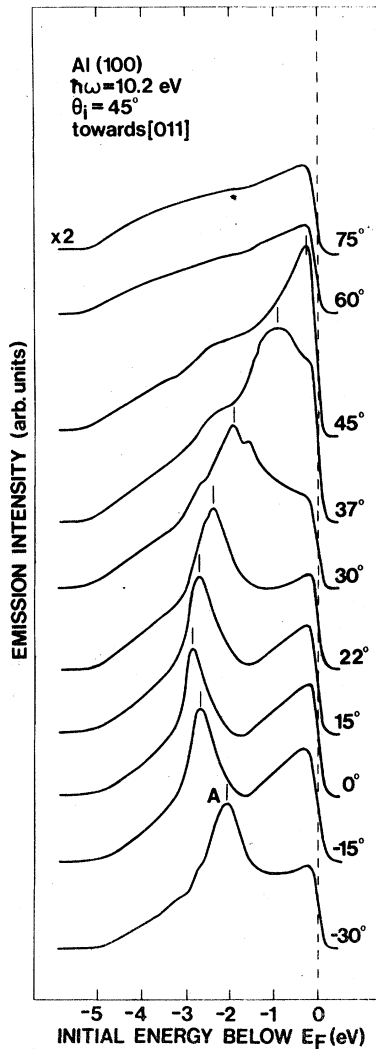


FIG. 2. Photoemission spectra measured on the (100) crystal face for different polar angles in the (011) plane.

emission angle are indicated. Also drawn are the three lowest energy bands along the line in  $\vec{k}$  space containing the X-point and parallel to both the (100) plane and one of the symmetry planes. The left-hand side shows the peak position and the bands in the (010) plane, which in the two-dimensional Brillouin zone corresponds to going from  $\bar{\Gamma}$  towards  $\bar{M}$ . At about  $0.75 \text{ \AA}^{-1}$ , the band gap is intersected by the band originating from the (1,1,1) or (1,-1,1) point in the repeated-zone scheme. This band does not, however, mix with the other two since it has different symmetry ( $\bar{\Sigma}_2$  vs  $\bar{\Sigma}_1$ ). In agreement with theory, the experiments give a dispersion curve reaching up to the Fermi level. There are no changes in the spectra which can be attributed to mixing.

The right-hand side of Fig. 3 shows the peak

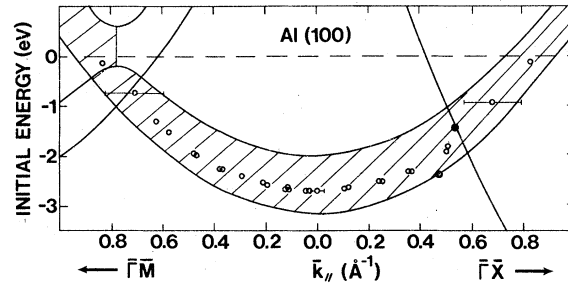


FIG. 3. Dispersion of peak A in emission from the (100) crystal face (rings), the extra structures in the spectrum for  $\theta_e = 30^\circ$  are included (dots). Also drawn are the three lowest bulk energy bands showing the  $sp$  band gap around the X point.  $\vec{k}_{\parallel}$  is in the [001] direction on the left-hand side of the figure, and in the [011] direction on the right-hand side.

position and the projected bands in the (011) plane. In contrast to Caruthers *et al.*,<sup>4</sup> we have chosen to draw the bands assuming the mixing is negligible. The reason for doing this is primarily to show where one can expect to see surface resonances if the induced mixing between bulk bands at the surface is small. Figure 3 thus shows an absolute band gap for  $|\vec{k}_{\parallel}| < 0.5 \text{ \AA}^{-1}$  in the  $\bar{\Gamma}\bar{X}$  direction while there is a "filled band gap" for  $|\vec{k}_{\parallel}| > 0.5 \text{ \AA}^{-1}$ . Experimentally, we see strong emission in the region of the "filled band gap" where there should be no surface states according to Caruthers *et al.*<sup>4</sup> We interpret this as emission from a surface resonance band, which from an experimental point of view is comparable to the surface-state band. Neither intensity nor dispersion is drastically different in the two regions. We see, however, indications of mixing in the shape of the spectra in Fig. 2. For  $\theta_e = 30^\circ$ , there is one structure on either side of the main peak. These structures are seen in a very narrow angle interval that corresponds fairly well to the value of  $\vec{k}$  at which band No. 3 crosses the band gap in the three-dimensional  $\vec{k}$  space. The reason why only one extra structure is seen in the  $\theta_e = -30^\circ$  spectrum is probably the uncertainty in the polar angle setting. The change in the AREDC's from  $\theta_e = 22^\circ$  to  $\theta_e = 30^\circ$  is very drastic, and the  $\theta_e = -30^\circ$  spectrum seems to correspond to an intermediate angle. In Fig. 3 the extra structures are marked as dots which are within  $0.1 \text{ \AA}^{-1}$  from the crossing of the band gap. The large half-width of the peak at  $\theta_e = 37^\circ$  is due to the finite angular resolution. Note that these extra structures were not seen in emission in the (010) plane, where mixing is possible only very close to the Fermi level.

Several authors have measured the yield as a function of photon energy from polycrystalline or single-crystal aluminum. They report a drastic

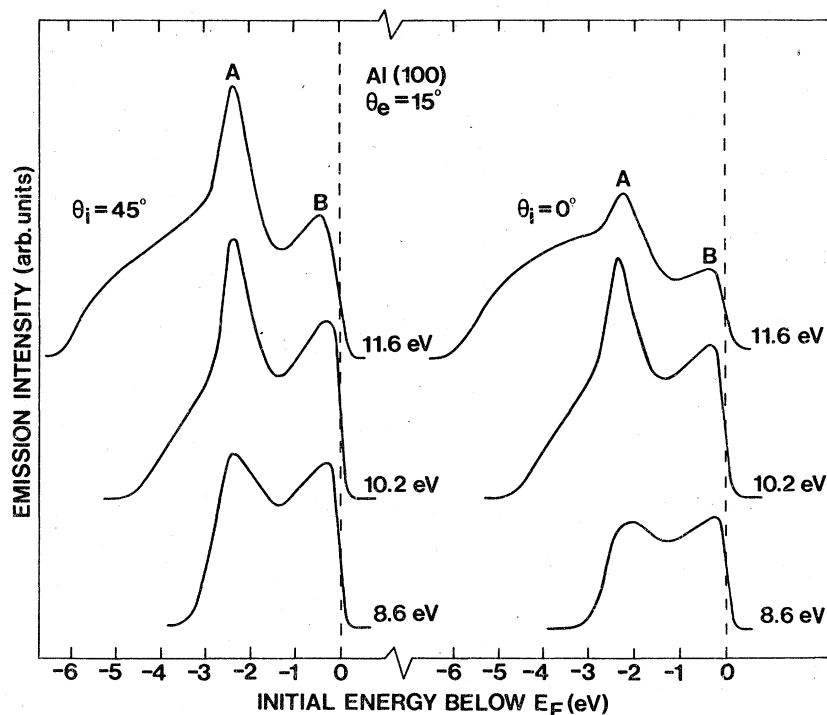


FIG. 4. Emission at  $15^\circ$  polar angle from the (100) crystal face. Comparison between the dependence on angle of light incidence at different photon energies.

increase in the yield close to the surface-plasmon energy, due to emission of electrons by surface-plasmon deexcitation.<sup>8,9,21</sup> The creation of surface plasmons is mediated by surface imperfections and is insensitive to the polarization and angle of incidence of the incoming light. Emission of electrons can thus be obtained through two different excitation fields: excitation by the surface-plasmon field or excitation by the normal optical field. Both fields can excite electrons through the bulk potential (direct transitions), through the surface potential or through the variation in the  $\vec{A}$  vector at the surface. The surface photoemission from the normal optical field is very sensitive to the polarization of the incident light due to the selection rules for an optical transition.

At 8.6 or 11.6 eV, the yield due to surface-plasmon decay is low.<sup>8,9,21</sup> Figure 4 shows the strong decrease in both structures A and B when changing the angle of incidence from  $45^\circ$  to  $0^\circ$ . This indicates surface photoemission through the normal optical field at these photon energies. At 10.2 eV, one is close to the maximum in yield due to surface-plasmon decay and the AREDC's are indeed found not to be very sensitive to the angle of light incidence, i.e., the polarization (Fig. 4). The intensity of emission from initial energies below the surface-state energy is quite insensitive to the light polarization even at 11.6-eV photon energy. This is not clearly understood, but we suggest that

it is due to emission from the bulk. We also note that low-energy emission increases very sensitively with contamination.

#### B. Al(111)

The normal emission from Al(111) for different photon energies has very little structure. Just like from Al(100), there is a region close to the Fermi level with an intensity which is almost linearly increasing with energy. The variation of the AREDC's with polar angle in the (01 $\bar{1}$ ) plane is shown in Fig. 5. For  $\theta_e < 45^\circ$  there is no sharp structure, but at about  $\theta_e = 50^\circ$  a peak C is seen near the Fermi level. This peak moves downward in energy with increasing angle. The dispersion<sup>24</sup> of peak C is plotted in Fig. 6 together with the projection of the bulk energy bands in the (100) plane going through the X point. For all angles, the position of peak C is within the projection of the band gap, i.e., peak C may be due to emission from a surface resonance in that band gap. We denote it by surface resonance, since there are projected bulk bands crossing over the band gap. We also compare it with the calculated polar angle dependence of the contributions due to direct transitions. In Fig. 6 the dispersion of direct transitions between bands Nos. 2 and 3 invoking the  $\vec{C}_{200}$  reciprocal-lattice wave vector is shown by the dotted line. This primary cone<sup>16</sup> emission is also a pos-

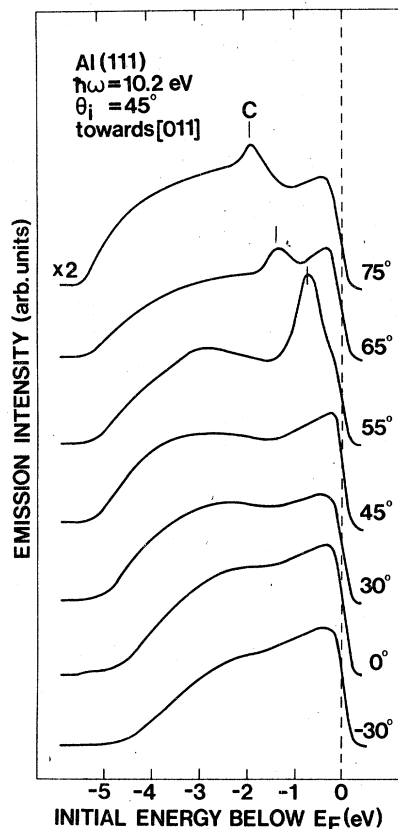


FIG. 5. Photoemission spectra for an Al(111) surface. The polar angle is varied in the (011) plane.

sible explanation of peak C.

To clarify the origin of peak C, we have performed the traditional tests for surface states, i.e., sensitivity to light polarization, gas adsorption, and disordering of the surface. The emission at  $\theta_e = 75^\circ$ , with angles of light incidence of  $45^\circ$  and  $0^\circ$ , respectively, is shown in Figs. 7(a) and 7(b). Both peak C and the emission close to the Fermi

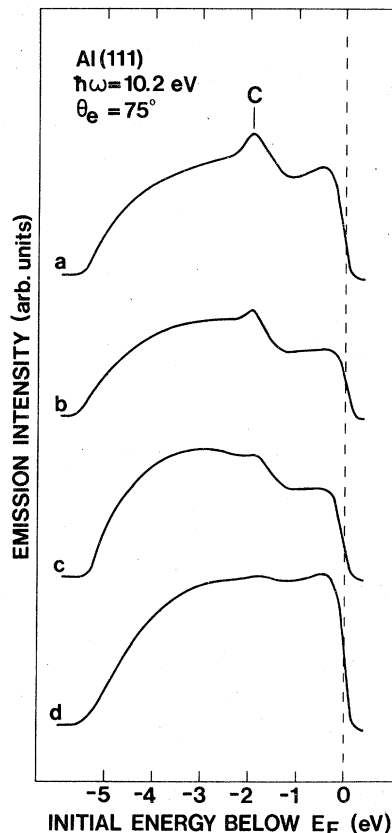


FIG. 7. Emission from the (111) surface at a polar angle of  $75^\circ$ . The analyzer is in the (011) plane, near the [100] direction ( $\theta_{100} = 54.7^\circ$ ). (a) Clean annealed surface,  $\theta_i = 45^\circ$ . (b) Clean annealed surface,  $\theta_i = 0^\circ$ . (c) After exposure to 100 L of  $O_2$ ,  $\theta_i = 45^\circ$ . (d) Disordered surface through argon sputtering,  $\theta_i = 45^\circ$ .

level are decreased for  $\theta_i = 0^\circ$ , indicating emission from the surface. This decrease is stronger than the corresponding decrease in the emission from the (100) crystal face at the same photon energy. As mentioned earlier, the deexcitation of surface plasmons gives a considerable contribution to the emission at 10.2 eV photon energy, that is only weakly dependent on the polarization. The strength of this mechanism depends on the degree of surface roughness and it has been shown that our cleaning procedure gives (111) surface that are smoother than the (100) surfaces.<sup>25</sup> The polarization dependence in Fig. 7 thus shows that we have noticeable excitation through the  $\vec{A}$  vector of the incoming light and that the intensity of peak C depends on the polarization.

Figure 7(c) shows the effect of exposure to 100 langmuir (one langmuir =  $10^{-6}$  Torr sec) of  $O_2$ , corresponding to 0.6–0.8 monolayer of oxygen.<sup>11</sup> The intensity of peak C is greatly reduced, while we get an increase in the low-energy part of the

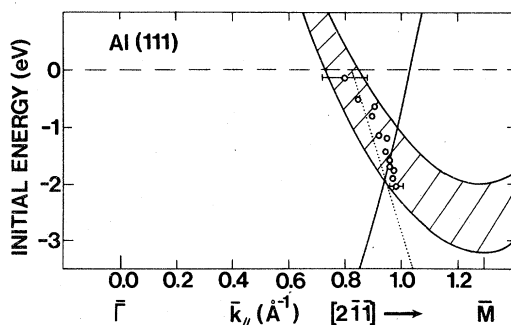


FIG. 6. Dispersion of peak C in emission from the (111) surface. This is compared with the projection of the band gap around the X point onto the (111) plane. The dotted line is the calculated variation of the peak position for direct transitions between band Nos. 2 and 3.

spectrum. Finally, in Fig. 7(d) we show the emission from the Al(111) surface after 12 min sputtering with argon ions at 600-eV kinetic energy with approximately  $10 \mu\text{A}/\text{cm}^2$  ion-beam current. After this disordering, peak *C* is hardly detectable and in addition the intensity near the Fermi level has increased. Annealing the surface at  $350^\circ\text{C}$  for 1 h restores order and the AREDC changes back to its original shape as in Fig. 7(a).

The value of the polarization-dependence test is always doubtful, but the sensitivity to oxygen exposure and sputtering leads us to assign peak *C* as being due to a surface resonance.<sup>26</sup> A rigid test of the existence of this surface resonance would be to measure on an Al(311) crystal face, from which the emission from the surface resonance should be clearly separable from any bulk contributions.

### C. Al(110)

The normal emission from the Al(110) crystal face for different photon energies is shown in Fig. 8. In contrast to the results for emission from the

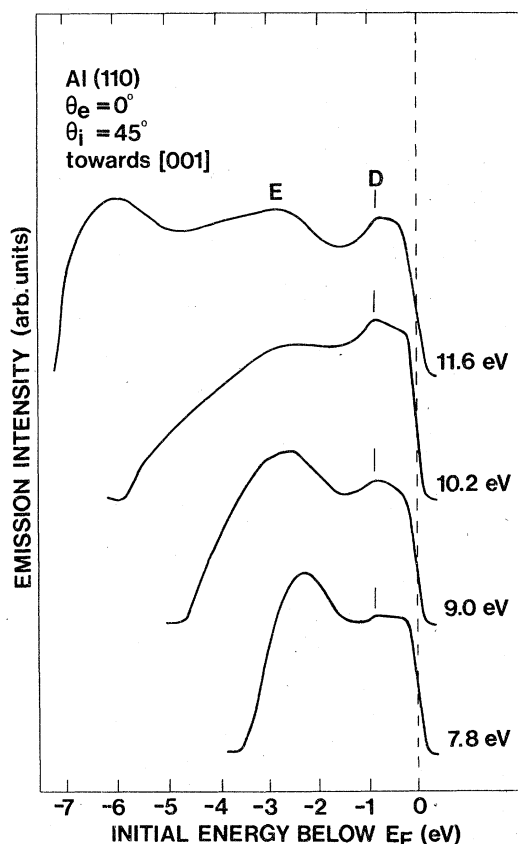


FIG. 8. Experimental spectra of photoelectrons emitted normal to the Al(110) surface for photon energies between 7.0 and 11.6 eV.

(100) and (111) crystal faces, we do not get the linearly increasing intensity close to the Fermi level. Instead, we get a small structure *D* at about  $-0.9$  eV for all photon energies, which indicates an initial-state effect. Between *K* and *X* in the  $\Gamma K$  direction there is a band gap, because of the mixing of the two bands with  $\Sigma_1$  symmetry. The midpoint of this gap is at  $-1.1$  eV in our calculation, while Caruthers *et al.*<sup>5</sup> find the band gap between  $-0.44$  and  $-0.83$  eV. We interpret structure *D* as the surface state predicted by Caruthers *et al.*<sup>5</sup> in the  $\bar{\Gamma}$  point gap. This surface state moves across the Fermi level with increasing angle in agreement with our results. There is also a broad structure *E* between  $-2.0$  and  $-3.5$  eV seen at normal emission. It has a minimum in intensity at  $10.2$ -eV photon energy. There are many possible contributions to this peak. Our calculation of direct transitions shows that within an angle  $\pm 7^\circ$  from the normal we can have transitions between bands 1-4, 1-5, 1-6, 2-4, 2-5, and 2-6 in this energy region. Also there are energy gaps in the regions of both initial and final states.

The selection rules for photoemission in the  $[110]$  direction say that the  $\Sigma_1$  initial states can only be excited by an  $\bar{A}$  vector in the normal direction  $[110]$ , while the  $\Sigma_3$  states are excited with the  $\bar{A}$  vector in the  $[001]$  direction.<sup>27</sup> Now, surface plasmons can be considered as *p*-polarized light near grazing incidence. This means that at  $10.2$ -eV photon energy the emission from  $\Sigma_1$  states should increase, while emission from the  $\Sigma_3$  states should decrease as compared to emission at the other photon energies used. Since structure *D* has a maximum and peak *E* a minimum at  $10.2$ -eV photon energy, we conclude that the initial states are  $\Sigma_1$  states for structure *D* and  $\Sigma_3$  states for peak *E*. This is consistent with our interpretation that *D* is a surface state in the band gap between  $\Sigma_1$  states and having the same  $\Sigma_1$  symmetry. We interpret peak *E* as photoemission from the lowest band, which has a saddle point near  $-3.2$  eV at *X*. The electronic states in this band have the correct  $\Sigma_3$  symmetry.

The polar angle dependence of the AREDC's in the (001) plane is shown in Fig. 9. The low-energy portions of the spectra are left out, since they were distorted due to a short circuit between the entrance slit and one cylindrical segment in the analyzer. This error changes the intensity of the parts of the spectra shown by less than 10%.<sup>28</sup> For emission angles  $|\theta_e| \geq 30^\circ$ , there is a peak *F* moving downwards in energy with increasing angle. This peak was very sensitive to oxygen exposure. The peak energy position as a function of the parallel momentum  $\bar{k}_\parallel$  is shown in Fig. 10, assuming a work function of  $4.28$  eV.<sup>24</sup> Also shown are the

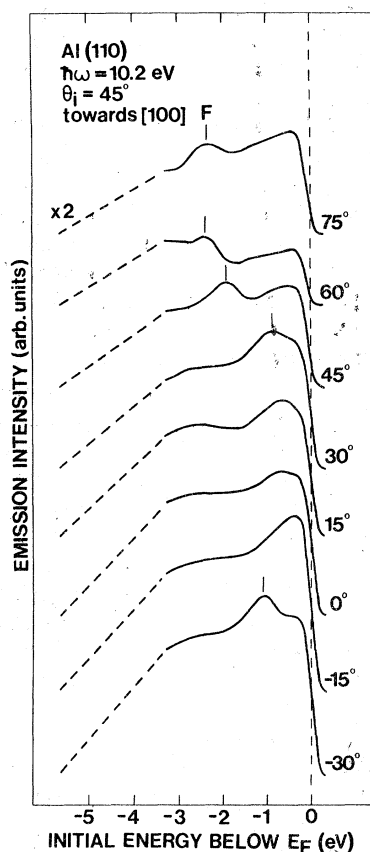


FIG. 9. Photoemission spectra measured on the Al (110) surface for different polar angles in the (001) plane.

projections of the bulk bands in the (100) plane going through the  $X$  point in  $\vec{k}$  space.  $\vec{k}_{||}$  is in the  $KW$  direction in the three-dimensional Brillouin zone. The dispersion of peak  $F$  is in agreement with the extension of the band gap centered at the  $X$  point which corresponds to  $\vec{k} \approx 1.1 \text{ \AA}^{-1}$ . A surface state in this band gap has been predicted in the calculation by Caruthers *et al.*<sup>5</sup>

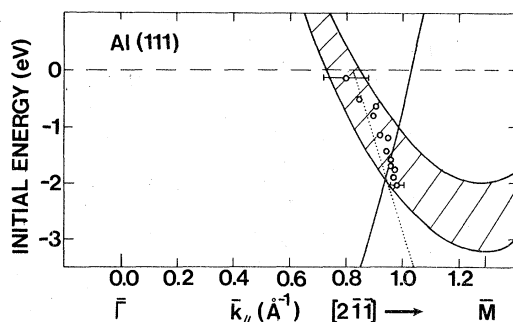


FIG. 10. Dispersion of peak  $F$  in emission from the (110) crystal face. This is compared with the projection of the band gap around the  $X$  point onto the (110) plane.

The angular variation of peaks due to direct transitions has been calculated for emission from the Al(110) crystal face. This shows that structures  $D$  and  $F$  cannot be accounted for as direct transitions.

## V. DISCUSSION

In the photon energy range used the photoemission from aluminum is a very complex process. There are two different excitation fields which can give emission: the normal optical field and the surface-plasmon field. Both fields can excite electrons through the gradients in the bulk potential  $\vec{\nabla}V_B$ , and surface potential  $\vec{\nabla}V_s$ , or through the variation of the vector potential at the surface  $\partial\vec{A}/\partial z$ . There are also cross terms which give important interference effects between the different contributions.<sup>29</sup> The relative importance of the optical and the surface-plasmon fields varies with photon energy. The main difference between them is the direction of the  $\vec{A}$  vector: the surface-plasmon field is always  $p$ -polarized, while the polarization of the normal optical field is variable. There is also a difference in the probing depths for the two excitation fields. The surface-plasmon field is more localized to the surface than is the normal optical field,<sup>21</sup> thus increasing that part of the emission related to the surface density of states.

The theoretical calculation by Pendry<sup>20</sup> shows that even for a constant optical field the main contribution to the emission is due to surface photoemission, i.e., the electrons are excited by the component of the  $\vec{A}$  vector normal to the surface. The effect of the surface-plasmon field is to increase the numbers of electrons excited by surface photoemission, but the energy positions of structures in the density of states probed will not change.

If we were probing the bulk density of states (DOS), we would expect to see sharp band edges near the band gaps. For example, the states at the band edges in the  $[100]$  direction have  $\Delta_1$  symmetry and they could, according to the selection rules, be excited by  $p$ -polarized light in a surface or bulk photoemission process. Gartland and Slagsvold<sup>2</sup> have assigned structures in the AREDC's at 16.8 eV photon energy to emission from the band edges. In their 11.8 eV spectrum one edge can be seen, while we see no sign of band edges at all in the photon energy range 7.0–11.6 eV. We believe that this is due to the extreme surface sensitivity of the surface photoemission process, particularly near the surface-plasmon energy.

It has been shown that the surface DOS at a band edge in the tight-binding approximation is less than



TABLE I. Effective mass, in units of the free-electron mass, for the three surface states or resonances assigned to the band gap around the  $X$  point.  $m_1^*$  and  $m_2^*$  are effective masses for the projections of the bulk bands at  $X$ .

| Crystal face | Peak | $m^*$           | $m_1^*$ | $m_2^*$ |
|--------------|------|-----------------|---------|---------|
| (100)        | $A$  | $1.02 \pm 0.05$ | 1.08    | 1.18    |
| (111)        | $C$  | $0.32 \pm 0.06$ | 0.36    | 0.39    |
| (110)        | $F$  | $0.6 \pm 0.1$   | 0.54    | 0.59    |

in the bulk.<sup>30,31</sup> Caruthers *et al.*<sup>4</sup> did not calculate the DOS's in the different layers in their thin-film calculations. The energy bands they reported for the 13-layer (100) aluminum film show larger band gaps than in the bulk calculation. It can also be inferred from the energy bands they show that there are no peaks in the DOS at the band edges in the film calculations. The distance between adjacent bands below the band gap at  $\bar{\Gamma}$  increases monotonically with energy all the way up to the band gap. Since the energy bands of the film give an integrated DOS over the whole volume, we expect the DOS at an Al(100) surface to differ even more from the bulk DOS.

The emission from the Al(100) crystal face, as calculated by Pendry, was mainly due to the surface-potential term, which probes the density of states at the surface for a certain  $\vec{k}_{||}$ . In full agreement with our experimental results, there are no structures due to the band edges of the bulk bands in his calculation. There is also agreement between our experimental results and Pendry's calculation with respect to the shape of the AREDC's. The AREDC's have a nearly linearly increasing part near the Fermi level, giving a minimum in the intensity on the high-energy side of the surface-state peak. The low-energy side of the surface-state peak is very slowly decreasing and the in-

tensity is much higher than one would get from an extrapolation of the intensity near the Fermi level.

Four structures have been assigned to emission from surface states or surface resonances. Three of them ( $A$ ,  $D$ , and  $F$ ) have earlier been predicted as surface states in theoretical calculations. The experimental dispersion of peak  $A$  extends outside the calculated surface state region, where it is interpreted as a surface resonance. Peak  $C$  has no counterpart in the theoretical calculations, but the dependence on oxygen exposure and disordering leads to the conclusion that it is a surface resonance. The dispersion of peak  $C$  coincides with the projection of the band gap between the two lowest bands at the  $X$  point, just as for peaks  $A$  and  $F$ .

We have calculated the effective mass  $m^*$  for the surface states or surface resonances assuming a parabolic dispersion:

$$E = E_0 + \hbar^2(k_{||} - k_{0||})^2/2m^*. \quad (4)$$

A least-squares fit to the experimental values was made assuming that  $E_0 = 2.75$  eV and that  $\vec{k}_{0||}$  equals the projection of the  $\Gamma X$  vector onto each plane. The effective masses are compared in Table I with the corresponding effective masses  $m_1^*$  and  $m_2^*$  for the projection of the two bulk bands giving the band gap around the  $X$  point.

To summarize, we state that the angular-resolved photoemission from aluminum single crystals is dominated by surface photoemission at photon energies below 11.6 eV. Depending on the photon energy, this surface photoemission is due to the normal optical field or the surface-plasmon field. The surface-plasmon field, being  $p$ -polarized, increases the yield due to surface photoemission. Independent of the details of the excitation field, structures seen in the spectra reflect the surface DOS.

Four structures have been assigned to emission

TABLE II. Summary of predicted and experimentally observed surface states and surface resonances.

| Crystal face | Peak | Location in two-dimensional Brillouin zone | Theoretical predictions             | Experimental interpretations    |                 |
|--------------|------|--|-------------------------------------|---------------------------------|-----------------|
|              |      |  | Caruthers <i>et al.</i> (Refs. 4-6) | Gartland and Slagsvold (Ref. 2) | Present work    |
| (100)        | $A$  | $\bar{\Gamma} \rightarrow \bar{M}$         | state                               | state                           | state           |
| (100)        | $A$  | $\bar{\Gamma} \rightarrow \bar{X}$         | state                               | state, resonance                | state resonance |
| (111)        | ...  | $\bar{\Gamma} \rightarrow \bar{M}$         | state                               | ...                             | ...             |
| (111)        | $C$  | $\bar{M} \rightarrow \bar{\Gamma}$         | ...                                 | ...                             | resonance       |
| (110)        | $D$  | $\bar{\Gamma} \rightarrow \bar{X}$         | state                               | ...                             | state           |
| (110)        | $F$  | $\bar{X} \rightarrow \bar{\Gamma}$         | state                               | ...                             | state           |

from surface states or surface resonances. Table II shows a summary of our interpretation of these structures together with theoretical predictions. We have included only predicted surface states which can be studied with photon energies below 11.6 eV. One predicted surface state on the (111) crystal face has not been observed, probably since it is too close to the low-energy edge of our spectra.

#### ACKNOWLEDGMENTS

The authors are indebted to S. Persson for calculating the band structure and the angular dependence of direct transitions. We also thank Professor S.-E. Karlsson for his support and interest in this work. This project has in part been financially supported by the Swedish National Science Research Council (NFR).

- <sup>1</sup>*Photoemission and the Electronic Structure of Surfaces*, edited by B. Feuerbacher, B. Fitton, and R. F. Willis, (Wiley, London, 1978).
- <sup>2</sup>P. O. Gartland and B. J. Slagsvold, *Solid State Commun.* **25**, 489 (1978).
- <sup>3</sup>D. S. Boudreaux, *Surf. Sci.* **28**, 344 (1971).
- <sup>4</sup>E. B. Caruthers, L. Kleinman, and G. P. Alldredge, *Phys. Rev. B* **8**, 4570 (1973).
- <sup>5</sup>E. B. Caruthers, L. Kleinman, and G. P. Alldredge, *Phys. Rev. B* **9**, 3325 (1974).
- <sup>6</sup>E. B. Caruthers, L. Kleinman, and G. P. Alldredge, *Phys. Rev. B* **9**, 3330 (1974).
- <sup>7</sup>J. R. Chelikovsky, M. Schlüter, S. G. Louie, and M. L. Cohen, *Solid State Commun.* **17**, 1103 (1975).
- <sup>8</sup>S. A. Flodström, G. V. Hansson, and S. B. M. Hagström, *Surf. Sci.* **53**, 156 (1975).
- <sup>9</sup>A. Quemerais, M. Priol, S. Megtert, B. Loisel, and S. Robin, *Opt. Commun.* **17**, 175 (1976).
- <sup>10</sup>S. A. Flodström, L.-G. Petersson, and S. B. M. Hagström, *Solid State Commun.* **19**, 257 (1976).
- <sup>11</sup>C. W. B. Martinsson, L.-G. Petersson, S. A. Flodström, and S. B. M. Hagström, European Space Agency Report No. ESA Sp-118, 1976 (unpublished), p. 177.
- <sup>12</sup>K. Y. Yu, J. N. Miller, P. Chye, W. E. Spicer, N. D. Lang, and A. R. Williams, *Phys. Rev. B* **14**, 1446 (1976).
- <sup>13</sup>J. G. Endriz, *Phys. Rev. B* **7**, 3464 (1973).
- <sup>14</sup>M. S. Chung and T. E. Everhart, *Phys. Rev. B* **15**, 4699 (1977).
- <sup>15</sup>E. C. Snow, *Phys. Rev.* **158**, 683 (1967).
- <sup>16</sup>G. D. Mahan, *Phys. Rev. B* **2**, 4334 (1970).
- <sup>17</sup>P. J. Feibelman and D. E. Eastman, *Phys. Rev. B* **10**, 4932 (1974).
- <sup>18</sup>B. Feuerbacher and R. F. Willis, *J. Phys. C* **9**, 169 (1976).
- <sup>19</sup>P. J. Feibelman, *Phys. Rev. Lett.* **34**, 1092 (1975).
- <sup>20</sup>J. B. Pendry, *J. Phys. (Paris)* (to be published), Daresbury report p. 82 (1977).
- <sup>21</sup>J. G. Endriz and W. E. Spicer, *Phys. Rev. B* **4**, 4159 (1971).
- <sup>22</sup>G. V. Hansson and S. A. Flodström, *Phys. Rev. B* **18**, 1572 (1978).
- <sup>23</sup>Contamination gave an increase of the low-energy parts of the spectra, while peaks assigned to surface states decreased.
- <sup>24</sup>We use the values of the work functions determined by J. G. Grepstad, P. O. Gartland, and B. J. Slagsvold, *Surf. Sci.* **57**, 348 (1976).
- <sup>25</sup>S. A. Flodström, R. Z. Bachrach, R. S. Bauer, and S. B. M. Hagström, *Proceedings of the Third International Conference on Solid Surfaces*, Vienna, 1977, (unpublished) p. 869.
- <sup>26</sup>It can be argued that the disturbance of the surface due to oxygen exposure or sputtering also will modify emission from the bulk, due to increased nonspecular surface scattering.
- <sup>27</sup>J. Hermanson, *Solid State Commun.* **22**, 9 (1977).
- <sup>28</sup>This was tested by measuring corresponding spectra from the (111) crystal face using both analyzer modes.
- <sup>29</sup>W. L. Schaich and N. W. Ashcroft, *Solid State Commun.* **8**, 1959 (1970).
- <sup>30</sup>D. Kalkstein and P. Soven, *Surf. Sci.* **26**, 85 (1971).
- <sup>31</sup>R. Haydock and M. J. Kelly, *Surf. Sci.* **38**, 139 (1973).